Oxidation of Ethane over Silica-Supported Alkali Metal Vanadate Catalysts

A. ERDÖHELYI AND F. SOLYMOSI

Reaction Kinetics Research Group of the Hungarian Academy of Sciences and Institute of Solid State and Radiochemistry, University of Szeged, P.O. Box 168, H-6701 Szeged, Hungary

The partial oxidation of ethane has been investigated on silica-supported alkali metal vanadate catalysts in a fixed-bed continuous-flow reactor at 770–823 K using N_2O as oxidant. Pulse experiments, temperature-programmed reduction of the catalyst, and catalytic decomposition of N_2O and C_2H_5OH were also carried out. The main products of the oxidation reaction were ethylene, acetaldehyde, CO, and CO_2. Small amounts of CH_4, C_2H_5OH, C_3-, and C_4-hydrocarbons were also identified. The introduction of water increased the acetaldehyde selectivity but decreased that of ethylene. In the presence of water the acetaldehyde selectivity increased from $LiVO_3$ to $RbVO_3$. Detailed kinetic measurements were carried out on KVO_3/SiO_2. From the pulse experiments it was inferred that in the oxidation of ethane an intermediate more reactive than C_2H_6 is formed for the activation of the catalysts. The temperature-programmed reduction spectra of alkali vanadates show that the onset temperature of the main reduction stage increased, while the extent of the reduction decreased somewhat from Li to Cs. A possible mechanism for the oxidation reaction is discussed.

INTRODUCTION

Vanadium oxides have been widely used as catalysts in various oxidation reactions. Their catalytic performance can be altered by alkali metal compounds as promoters. The efficiency of the latter generally decreases in the sequence Cs–Rb–K–Na–Li *(1–3)*. However, the sequence Li–Na–K–Rb–Cs has also been reported *(4–6)*.

It was recently shown that SiO_2-supported V_2O_5 and MoO_3 are effective catalysts for the oxidation of C_2H_6 by N_2O to C_2H_4 and acetaldehyde *(7–12)*. In a short paper we reported that the efficiency of V_2O_5/SiO_2 was markedly increased in the presence of K_2O *(11)*, but deactivation of the catalyst occurred rapidly. However, no significant decay in activity was observed for KVO_3. This prompted us to investigate the catalytic performance of KVO_3 in the oxidation of C_2H_6 in greater detail and to extend our studies to other alkali metal vanadates. The catalytic effects of alkali metal vanadates in different oxidation reactions have been studied in only a few papers *(6, 13–16)*.

EXPERIMENTAL

Materials. The catalysts were prepared by impregnation of the silica (Cab-O-Sil) support from a basic solution of different alkali metavanadates to yield a nominal 2 wt% of V_2O_5. The suspension was dried and heated at 823 K for 5 h. $LiVO_3$, $NaVO_3$, and KVO_3 were prepared by the solid-state reaction of alkali carbonates and V_2O_5 *(17)*. $RbVO_3$ and $CsVO_3$ were produced by the reaction of alkali metal carbonates with V_2O_5 in a hot solution *(17)*. Samples have been characterized by X-ray analysis which showed only the lines characteristic of alkali metal vanadates.

Before catalytic measurements, the sample was oxidized in O_2 flow for 1 h at 773 K in the reactor. After the oxidation the catalyst was heated to the reaction tempera-

TABLE 1

Some Characteristic Data of Silica-Supported Alkali Vanadates

	Melting point[a] (K)	$R_M{}^b$ (Å)	BET surface area (m²/g)	$O_2{}^c$ uptake (μmol/g)	D^d (%)	CO_2 uptake (μmol/g)	Irrev. ads.[e] (μmol/g)	Number of acidic sites (μmol/g)
V_2O_5/SiO_2	1073	—	112	86.8	83.7	27.9	—	49.3
$LiVO_3/SiO_2$	895	0.68	83	66.2	60.2	68.8	—	39.1
$NaVO_3/SiO_2$	899	0.97	99	16.3	20.1	88.8	3.9	38.9
KVO_3/SiO_2	795	1.33	110	33.5	30.5	90.6	7.5	33.4
$RbVO_3/SiO_2$	839	1.52	94	42.9	26.8	103.1	10.5	33.2
$CsVO_3/SiO_2$	918	1.70	102	18.1	16.4	110.6	21.2	32.7

[a] Melting point of catalyst.

[b] Ion radius of the alkali ion.

[c] The O_2 uptake determined at 641 K after reduction of the sample at 641 K.

[d] The amount of surface V ions, determined by O_2 adsorption at 641 K, assuming $O_{ads}/V_{surf} = 1$ (19).

[e] The amount of irreversibly bonded CO_2, characteristic for the number of basic sites.

ture in flowing He. Some characteristic data for the catalysts are shown in Table 1.

The reactant gases C_2H_6 (99.9%), N_2O (99.7%), and O_2 (99.9%) were used as received. He (99.9%) was purified with an Oxy-trap. Other impurities were adsorbed on a 5A molecular sieve at the temperature of liquid air.

Methods. The reaction was carried out in a fixed-bed continuous flow reactor (12, 18). Generally, we used 1 g catalyst. The reacting gas mixture consisted of 20% ethane, 40% oxidant, and He as diluent. When the effect of water vapour was studied, the gas mixture was saturated with water by bubbling it through preheated water. The space velocity was 20.000 h⁻¹. The products were analysed with a Hewlett–Packard 5750-type gas chromatograph using columns of Porapak QS and 5A molecular sieve. Conversions are defined as (moles ethane reacted per min)/(mol ethane fed per min). Selectivity S is defined as (mol products formed per min)/(mol ethane reacted per min).

The pulse reactor, made from an 8-mm-i.d. quartz tube, was incorporated between the sample inlet and the analytical column of the gas chromatograph. The dead volume of the reactor was filled with quartz beads.

Temperature-programmed reduction (TPR) experiments were carried out in the pulse reactor. The reactor was heated by an external oven at a linear rate of 40 K min⁻¹ to a final temperature of 1100 K. Nitrogen carrier gas was used which contained 10% of H_2, and the hydrogen consumption was determined by the gas chromatograph. Details of the TPR procedure have been described elsewhere (18).

Decomposition of N_2O was studied in the temperature range 620–720 K in a static reactor fitted with a gas recirculation system. The reaction was followed by the pressure change, and the gas phase was analysed by a mass spectrometer.

Decomposition of C_2H_5OH was investigated in the flow system. It was introduced into the reactor after bubbling He through absolute C_2H_5OH. The concentration of the alcohol in the He flow was usually about 10%. The amount of catalyst was 0.5 g.

BET areas of catalyst samples were measured by nitrogen adsorption at 77 K in a conventional volumetric apparatus. The number of surface V ions was determined by the method developed by Oyama *et al.* (19). This is based on measuring the oxygen uptake at 640 K on samples reduced in H_2 at the same temperature. It is assumed that at this temperature only the surface V=O

groups are reduced and the ratio of O_{ads}/V_{surf} is 1.

The number of basic sites has been determined by the method of Ai (20). This involves the adsorption of CO_2 at room temperature. The number of acidic sites was measured by n-butylamine titration (21).

RESULTS

1. Oxidation of C_2H_6 on KVO_3/SiO_2

The catalyst was treated with the reacting gas mixture at the highest reaction temperature, usually 823 K. In the catalytic reaction, CO, CO_2, C_2H_4, CH_3CHO, a small amount of CH_4, C_3- and C_4-hydrocarbons, and C_2H_5OH were detected. There was no or very little change in the conversion and product distribution during the conditioning period (Fig. 1). The conversion of C_2H_6 at 823 K was about 11%, and the selectivities for C_2H_4 and CH_3CHO production were about 34 and 7.5%, respectively. The amount of N_2O reacted corresponded well to that of the products that required oxygen. When the temperature was lowered, the conversion decreased, but the selectivities for C_2H_4 and CH_3CHO formation increased (Fig. 1B). The activation energy for the ethane consumption was found to be 108.5 kJ/mol.

The introduction of H_2O into the reacting gas mixture somewhat decreased the C_2H_6 conversion and the rate of product formation. However, the selectivities for CH_3CHO formation increased with increasing H_2O concentration (Fig. 2). The highest value for S_{CH_3CHO} was about 21% at a conversion of 4% at 803 K.

The conversion of C_2H_6 and the rates of formation of all products increased with elevation of the N_2O concentration (5–60%), but the selectivity of CH_3CHO formation decreased (Fig. 3). When the N_2O content of the reacting gas mixture was 5%, the CH_3CHO selectivity was 46% at a C_2H_6 conversion of 0.3%.

The rates of the product formation showed a maximum as a function of C_2H_6 concentration (10–50%) at a C_2H_6 content
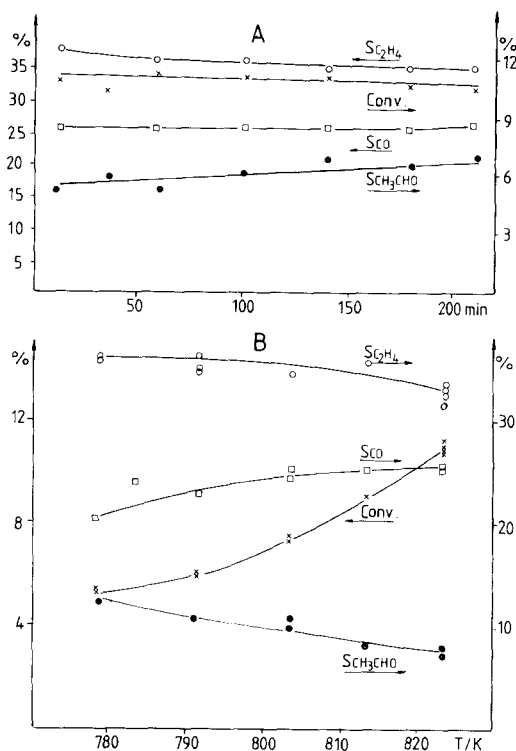

FIG. 1. (A) Change of the C_2H_6 conversion, the CH_3CHO, C_2H_4, and CO selectivity at 823 K on KVO_3/SiO_2. (B) Temperature dependence of the C_2H_6 conversion and the selectivity for CH_3CHO, C_2H_4, and CO formation. The concentration of C_2H_6 and N_2O was 20 and 40%, respectively.

of about 30%. The conversion of C_2H_6 decreased, but the CH_3CHO selectivity increased slightly with increasing C_2H_6 concentration (Fig. 4).

In order to establish the rate equation for the C_2H_6 conversion, the order of reaction was determined from a plot of the logarithm of the rate of C_2H_6 conversion vs the logarithms of the partial pressures of C_2H_6 and N_2O. It was found that the overall rate of C_2H_6 conversion can be described by

$$d(C_2H_6)/dt = k(C_2H_6)^{0.6}(N_2O)$$

over the range of concentration $10 \leq C_{C_2H_6} \leq 30\%$, and $6 \leq C_{N_2O} \leq 60\%$.

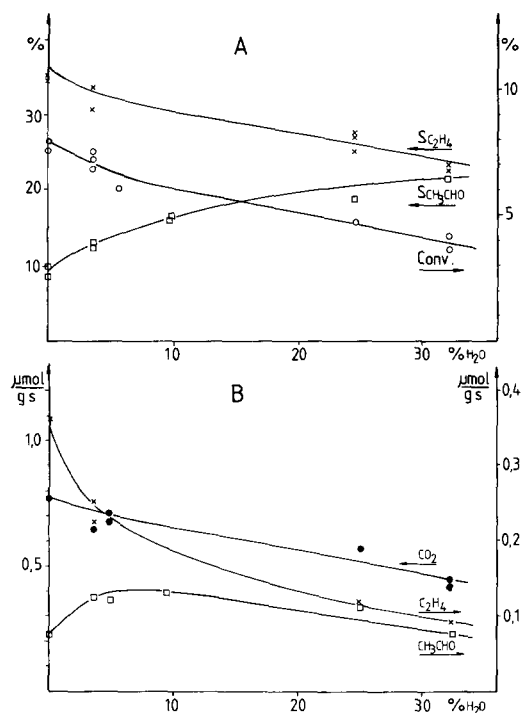The kinetic orders of reaction products have been determined in a similar way. Log-

FIG. 2. (A) The conversion, the CH_3CHO and C_2H_4 selectivity and (B) the rate of the product formation as a function of water concentration at 803 K on KVO_3/SiO_2. The concentration of C_2H_6 and N_2O was 20 and 40%, respectively.

arithmic plots of the various rates vs the volume percentage of the reactants are displayed in Figs. 3 and 4. We observed that the kinetic order with respect to N_2O is about 1.2 for all products except CH_3CHO up to 40% of oxidant. Above this concentration it was 0 for C_2H_4 formation. As concerns CH_3CHO production the order was 0.6 in the whole concentration range (Fig. 4).

The order with respect to ethane is 0.92 up to 30% for C_2H_4 and CH_3CHO formation. It was 0.4 for CO_2 and CO production. Above this concentration range the order was 0 for CH_3CHO and negative for CO_2 and C_2H_4 formation (Fig. 4). Data of these measurements are collected in Table 2.

The temperature-dependence of the reaction was also determined in the presence of

H_2O at 781–823 K. The results are shown in Fig. 5. The C_2H_6 conversion varied in the range 1.3–7.7%. The CH_3CHO selectivity increased with decreasing temperature; at 781 K it was about 50% at a conversion of 1.8%. An opposite change was observed for the selectivities for C_2H_4 and CO_2. The activation energy for ethane consumption was estimated to be 188.4 kJ/mol, which is considerably higher than that obtained under dry conditions.

2. Pulse Experiments

In the subsequent measurements, the reaction was investigated by means of a pulse technique. One pulse contained 20.8 μmol C_2H_6. The amount of catalyst was 0.32 g. Before the measurements, the catalyst was
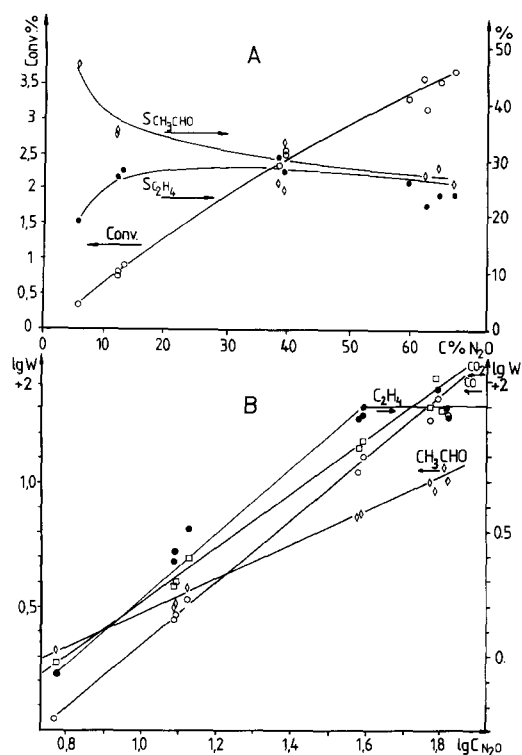

FIG. 3. (A) Dependence of the conversion, the CH_3CHO and C_2H_4 selectivity, and (B) the rate of the product formation as a function of N_2O concentration at 803 K on KVO_3/SiO_2. The C_2H_6 and H_2O content of inlet gas was 20%.
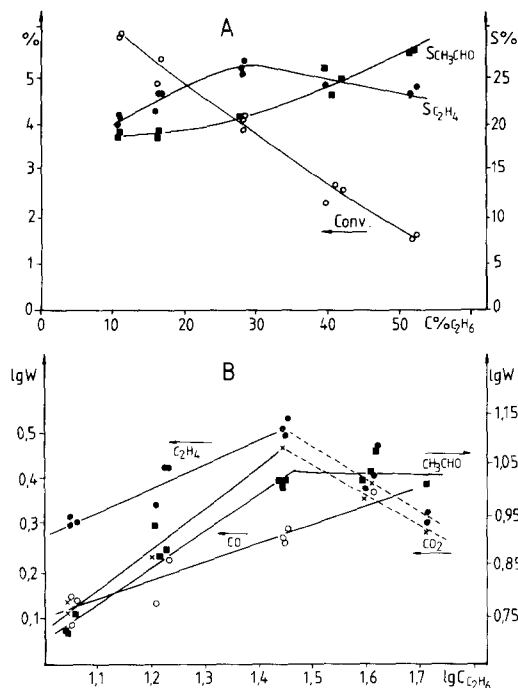
FIG. 4. (A) Dependence of the conversion, the CH_3CHO and C_2H_4 selectivity, and (B) the rate of the product formation as a function of C_2H_6 concentration at 803 K on KVO_3/SiO_2. The rate of formation of C_2H_4, CH_3CHO, CO, and CO_2 is multiplied by a factor of 100 and 10, respectively. The N_2O and H_2O content of inlet gas was 40 and 20%, respectively.

oxidized at 773 K then flushed with He and heated to 823 K in He stream.

First, the KVO_3/SiO_2 catalyst was treated at 823 K with pure C_2H_6. Only small amounts of carbon oxides (0.08 μmol CO_2 and 0.03 μmol CO) and C_2H_4 (0.04 μmol) were detected. After five C_2H_6 pulses, the catalyst adsorbed about 1.3 μmol O_2 at 823 K and only 0.015 μmol CO_2 was observed. Calculations showed that less than 0.3% of the C_2H_6 reacted with surface oxygen under these conditions. In harmony with this, only slight (0.5%) N_2O decomposition was observed on admission of a N_2O pulse onto oxidized KVO_3/SiO_2 at 823 K. This is in complete contrast with the behaviour of V_2O_5/SiO_2 catalyst when 3–3.5% C_2H_6 pulses reacted with the oxidized surface to give C_2H_4 (40–60%) and CH_3CHO (1%).

TABLE 2

Kinetic Data for the Ethane Oxidation on KVO_3/SiO_2 in the Presence of 20% Water Vapour

Products	Kinetic order			
	C_2H_6		N_2O	
	(a)	(b)	(c)	(d)
C_2H_4	0.9	−0.75	1.2	0
CH_3—CHO	0.9	0	0.6	0.6
CO	0.4	0.4	1.2	1.2
CO_2	0.4	−0.75	1.3	1.3

Note. (a) The order up to 28% C_2H_6 content at 803 K. (b) The order above 28% C_2H_6 content at 803 K, the N_2O concentration was 40%. (c) The order up to 40% N_2O content at 803 K. (d) The order above 40% N_2O content at 803 K, the C_2H_6 concentration was 20%.
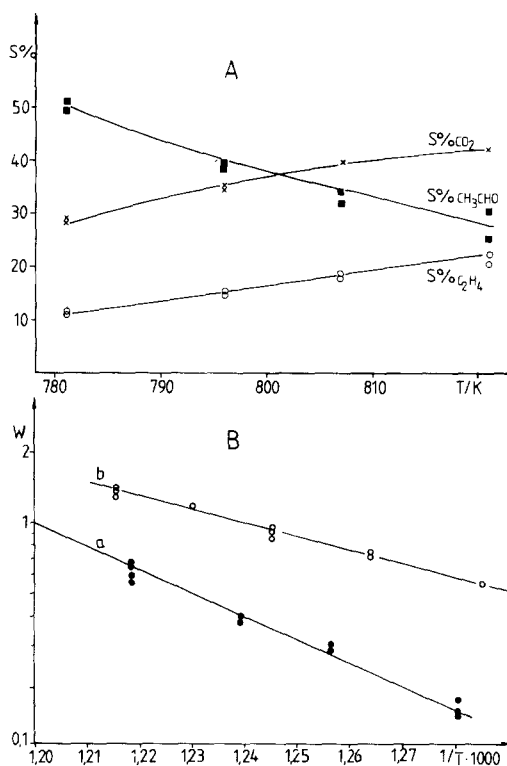

FIG. 5. (A) Temperature dependence of the selectivity for CH_3CHO, C_2H_4, and CO_2 formation. The concentration of C_2H_6, N_2O, and water was 20, 40, and 20%, respectively. (B) The Arrhenius plots for ethane consumption on KVO_3/SiO_2 in the presence (a) and in the absence (b) of 20% water vapour.
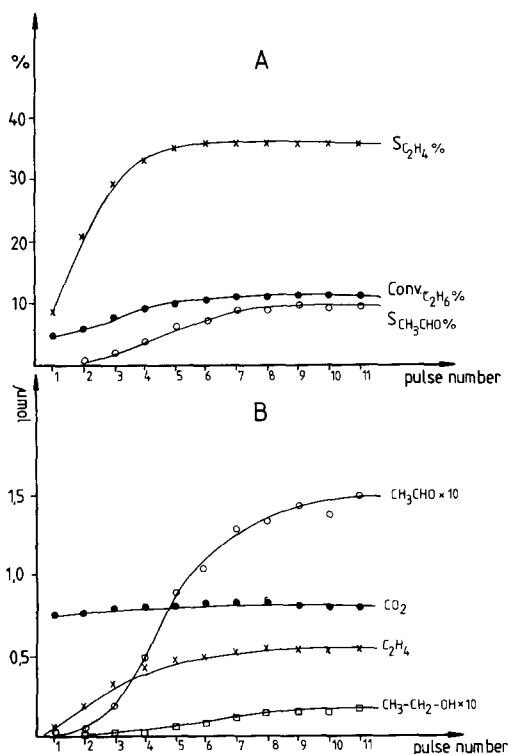
FIG. 6. (A) The conversion of C_2H_6, the CH_3CHO and C_2H_4 selectivity, and (B) the amount of the products formed in C_2H_6 + N_2O (1 : 1) pulse (20.8 μmol) on KVO_3/SiO_2 at 823 K.

On injection of a C_2H_6 + N_2O gas mixture (10.4 μmol C_2H_6 and 10.4 μmol N_2O) into the KVO_3/SiO_2 catalyst, CH_3CHO formation was detected only in traces in the first 2–3 pulses. However, its amount gradually increased and reached a steady value after 10–15 pulses, when the selectivity was about 10%. A more significant amount of C_2H_4 was produced. Its selectivity reached the maximum value, 36%, after only five pulses. The CO_2 formation changed only slightly as a function of the number of pulses. These results are shown in Fig. 6.

When O_2 or N_2O was admitted onto the sample at 823 K after the above experiments, only traces of CO_2 (0.018 μmol) were detected, and the catalyst adsorbed about 3.9 μmol O_2. Afterwards, the curve of CH_3CHO formation started from zero again (Fig. 7, curve a). When the catalyst was

reduced with five C_2H_6 pulses (the O_2 deficit was about 1.2 μmol), in the first gas mixture pulse somewhat more CH_3CHO was produced than on the untreated surface (curve b), but much less than after 10 C_2H_6 + N_2O pulses. In the latter case, the amount of CH_3CHO was 6–8 times higher. The largest initial value was obtained following the reduction of KVO_3/SiO_2 with CO (curve c) (the O_2 deficit was 6.3 μmol, which corresponds to a reduction of 5.9%). The amount of CH_3CHO formed in the first pulse was only a little less than that on the untreated surface in the 10th pulse. Similar behaviour was observed for the formation of C_2H_4.

3. Oxidation of C_2H_6 on Different Alkali Metal Vanadate/SiO_2 Catalysts

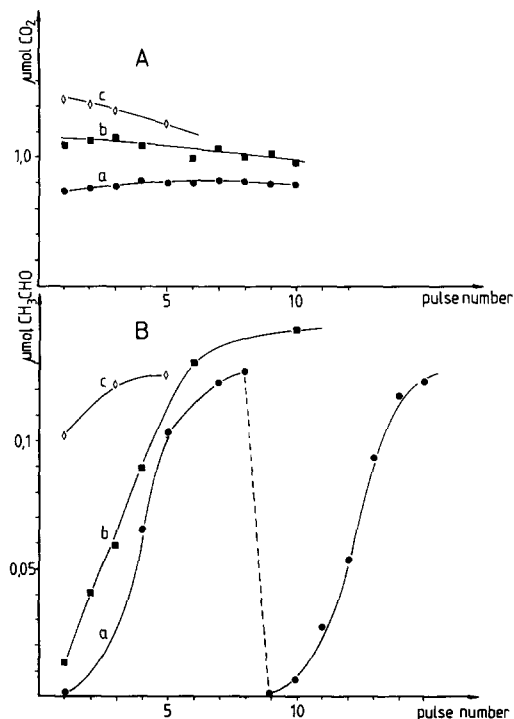In subsequent measurements, the oxidation of C_2H_6 was investigated on the other

FIG. 7. Amount of CO_2 (A) and CH_3CHO (B) formed in C_2H_6 + N_2O (1 : 1) pulses (20.8 μmol) on clean (a), with 104 μmol C_2H_6 (b), or with 20.8 μmol CO reduced KVO_3/SiO_2 at 823 K. In the case of curve (a) the sample was oxidized with N_2O after the eighth pulse.
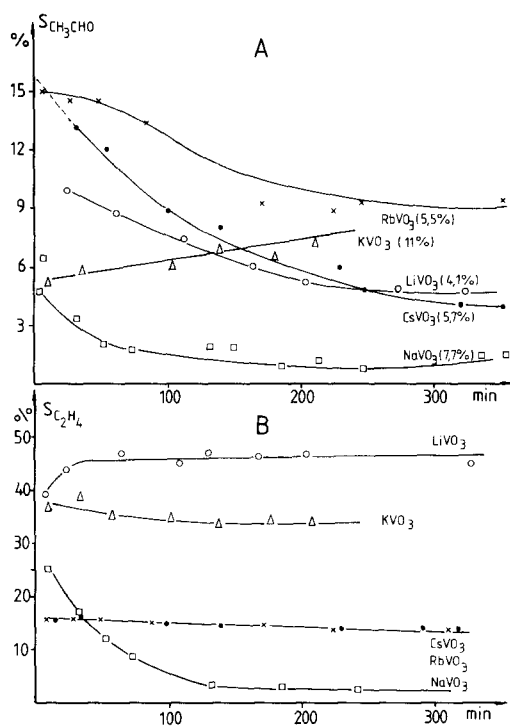
FIG. 8. The selectivity of CH_3CHO (A) and C_2H_4 (B) on different SiO_2-supported alkali metal vanadates at 823 K in the absence of water. The concentration of C_2H_6 and N_2O was 20 and 40%, respectively.

alkali metal vanadates. The reaction was carried out at 823 K, and the inlet gas mixture contained 20% C_2H_6 and 40% N_2O. The same products were identified as on KVO_3/SiO_2. At the beginning of the catalytic run (10 min), the rate of C_2H_6 consumption was in the range 8–12% and, in contrast with the situation on KVO_3, it decreased with time. Changes in the selectivities for C_2H_4 and CH_3CHO are illustrated in Fig. 8. The selectivity of C_2H_4 formation was the highest on $LiVO_3/SiO_2$ (40%) and it increased with time. The lowest value of the selectivity was observed on $CsVO_3/SiO_2$ and $RbVO_3/SiO_2$ (16.5%). No significant decay occurred with time except on $NaVO_3$, the activity of which decreased to a very low value after 2 h (1% conversion). The sequence of CH_3CHO selectivity was the opposite of this; the highest initial value was measured on $RbVO_3/SiO_2$ (15%) and the lowest (6.7%) on $NaVO_3/$

SiO_2. It is important to note that the initial activity of the catalysts could be regenerated by oxidation at 773 K. Some characteristic data are given in Table 3.

When the reacting gas mixture contained 20% H_2O vapour, the activities of the catalysts and the product distributions were different (Fig. 9). The most important feature is that the selectivity of CH_3CHO production was markedly enhanced on KVO_3, $RbVO_3$, and $CsVO_3$, and remained constant or even increased slightly with time. The decay in the activity of the catalysts was practically the same as observed in the absence of H_2O.

$NaVO_3/SiO_2$ was again an exception: in this case the conversion was 11.3% in the 10th min, and only about 1% after reaction for 6 h. The catalyst could not be reactivated by either oxidation or reduction. The BET surface area of the $NaVO_3/SiO_2$ catalyst, measured after the reaction, was less than 2 m^2/g. This feature was not observed for the other catalyst samples. When the temperature was lowered, the conversion decreased, but the selectivity for CH_3CHO formation increased greatly. In the case of $CsVO_3$, a value of 60% was attained at 781 K at a conversion of 1.4%.

4. Decomposition of N_2O on Alkali Metal Vanadates

For an interpretation of the effects of alkali metal vanadates on the partial oxidation of ethane, it is very useful to know their influence on the decomposition of N_2O. We have performed detailed kinetic measurements, the results of which will be published in a separate paper (22). The main observations pertaining to the present study are as follows: on alkali metal vanadates supported on silica and activated in vacuum at 703 K, the decomposition of N_2O occurs at well-measurable rates above 620 K. The products are N_2 and O_2 in a mol ratio of 2 : 1. The reaction followed first-order kinetics. Partial reduction at 673 K increased the rate of decomposition for all catalyst samples. Data for the catalytic activity of the vana-

TABLE 3

The Rate of C_2H_6 Consumption on Different Alkali Vanadate Catalysts at 823 K (Rates Measured at 10th Min)

	Conv. (%)	In the absence of H_2O		Conv. (%)	In the presence of 20% H_2O	
		$W_{C_2H_6}{}^a$ (μmol/g)	$W_{C_2H_6}{}^b$ (s^{-1})		$W_{C_2H_6}{}^a$ (μmol/g)	$W_{C_2H_6}{}^b$ (s^{-1})
V_2O_5/SiO_2	6.9	0.515	2.8×10^{-3}	5.2	0.375	2.04×10^{-3}
$LiVO_3/SiO_2$	10.2	0.94	7.1×10^{-3}	4.5	0.67	5.06×10^{-3}
$NaVO_3/SiO_2$	12.21	1.59	35.98×10^{-3}	11.3	1.86	42.09×10^{-3}
KVO_3/SiO_2	11.4	1.29	19.23×10^{-3}	9.2	1.15	17.14×10^{-3}
$RbVO_3/SiO_2$	8.58	1.17	19.85×10^{-3}	6.5	0.83	14.37×10^{-3}
$CsVO_3/SiO_2$	10.6	1.38	38.27×10^{-3}	7.0	0.91	25.22×10^{-3}

[a] The rate related to the amount of the catalysts.

[b] The rate related to the amount of the surface V atoms.

dates are shown in Table 4. The maximum activity was exhibited by $NaVO_3$.

5. Decomposition of Ethyl Alcohol on Alkali Metal Vanadates

Some exploratory measurements were also performed on the decomposition of ethanol. The aim was to establish the effects of alkali metal ions on the product distribution, and particularly on the ratio of ethylene and acetaldehyde. Decomposition occurred above 520 K. The rate of the decomposition of C_2H_5OH decreased from Li to Cs metavanadates. The main product was acetaldehyde (50–60%). A significant amount of ethane (33–43%) was identified, which always exceeded that of ethylene (3–6%). Traces (~1%) of CH_4, CO, and CO_2 were also detected. The ratio C_2H_x/CH_3CHO exhibited a little variance with alkali ions. Some data are presented in Table 5.

6. Reduction of Vanadates

As reduction and reoxidation of the surface of vanadates play an important role in the catalytic oxidation of hydrocarbons, the temperature-programmed reduction of vanadates was investigated. In previous studies, the addition of potassium salts to V_2O_5 increased the extent of reduction of V_2O_5. Monti et al. (23) found an increase by a factor of 2 on addition of K_2SO_4 to V_2O_5. Klissurski and Abadzhijeva (24) observed

that the effect of alkali metal sulphate increased in the sequence Li–Na–K–Rb–Cs. The mobility of oxygen in V_2O_5 was influenced in the same way.

TPR spectra of silica-supported vanadates are illustrated in Fig. 10. The hydrogen consumptions calculated from the TPR peak areas are shown in Table 6, which also contains characteristic data on the reduction. The onset temperature of the main reduction stage increased, while the extent of the reduction decreased somewhat in the sequence Li–Na–K–Rb–Cs. Nevertheless, there were no significant differences in the positions of the peak maxima, which lay in the narrow range 933–953 K for all samples. In the TPR spectra of Li and Na vanadates, low-temperature shoulders were observed. The average valency of vanadium after reduction is almost 3 for $LiVO_3$ and 4.4 for $CsVO_3$. The reduction of V_2O_5/SiO_2 started in a somewhat higher temperature range, but the peak maximum was practically the same as that for the alkali metal vanadates.

DISCUSSION

1. Properties of Alkali Metal Vanadates

Before a discussion of the catalytic results, it is useful to summarize some of the important properties of alkali metal vanadates, including their structures.
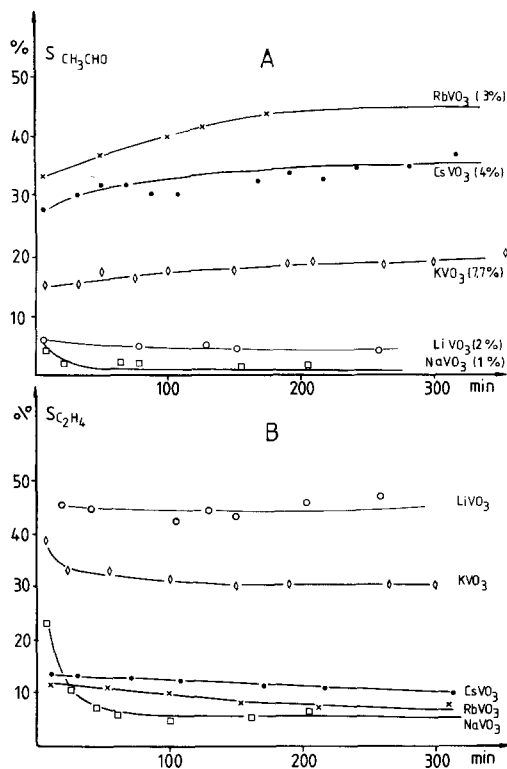
Vanadates can form metavanadates and

FIG. 9. The selectivity of CH_3CHO (A) and C_2H_4 (B) on different SiO_2-supported alkali metal vanadates at 823 K in the presence of water. The concentration of C_2H_6, N_2O, and water was 20, 40, and 20%, respectively.

polyvanadates. The two forms can be distinguished on the basis of their colours: alkali metal metavanadates (MVO_3) are usually white, whilst coloured compounds are probably polyvanadates. In these compounds, the amount of M_2O is less than that of V_2O_5. The colour of polyvanadates varies from yellow through red to brown (17).

$LiVO_3$ and $NaVO_3$ are monoclinic, with pyroxene-like structures with the space group $C2/c$ (25), KVO_3, $RbVO_3$, and $CsVO_3$ are orthorhombic with the space group $Pbcm$ (26). According to Bubnova and Filatova (27) KVO_3, $RbVO_3$, and $CsVO_3$ were also monoclinic.

The alkali metal vanadates are built up from chains of VO_4 tetrahedra connected by alkali metal cations. Each VO_4 grouping has two common oxygen atoms. In this struc-

ture the V–O distances differ significantly: the oxygen atoms that are common are involved in longer V–O bonds than the other atoms; the O–V–O angles differ from the tetrahedral value (109°25').

This is in contrast with V_2O_5, where the vanadium is in a bipyramidal environment. The structure is characterized by the presence of a short V–O bond (1.58 Å for V_2O_5). VO_4 tetrahedra are also found in the structure of V_2O_5, which contains relatively large channels. Through these channels, O_2 can pass into or out of the framework. The efficiency of V_2O_5 in oxidations is probably associated with these features. In the VO_4 tetrahedra there are two different V–O bond distances. (In V^{5+}, the $3d$ orbital is unfilled, but the $4s$ and $4p$ orbitals are rather near, and hybrid orbital formation is possible.) Metavanadates are built up from such tetrahedra, but the hydrated metavanadates consist of a bipyramidal structure with 5-coordination (28, 29).

Recently Mastikhin and co-workers (30) used ^{51}V and ^{29}Si NMR to study the KVO_3/SiO_2 system. They found that the vanadium near the surface is in an almost regular tetrahedral environment, but on interaction with H_2O it becomes octahedrally coordinated. It was inferred that the reaction between the vanadate and SiO_2 led to vanadium replacement in the tetrahedral oxygen environment (30).

The melting points of the alkali metal metavanadates lie in the temperature range 795–915 K, and change in the sequence Li = Na > K < Rb < Cs. Accordingly, KVO_3, with the lowest melting point (795 K), can melt on the surface of the support during catalytic reactions at 823 K. The other metavanadates melt without decomposition and are stable up to 1200 K. It has been reported that the heating of $NaVO_3$ to 720 K is accompanied by the release of O_2 and 3 Na_2O · V_2O_4 · V_2O_5 is formed; the colour changes from white to brown (31).

We have determined the number of surface acidic and basic sites of the catalysts (Table 1). It was found that the number of acidic sites on SiO_2-supported alkali metal

TABLE 4

Characteristic Data for the Decomposition of N_2O on SiO_2-Supported V_2O_5 and Alkali Metal Vanadates at 713 K

	k^a $(10^{-3}$ min$^{-1} \cdot$ g$^{-1})$	k^b $(10^{-5} \cdot$ min$^{-1} \cdot$ m$^{-2})$	k^c $(10^{-5} \cdot$ min$^{-1} \cdot$ V$_{atom}^{-1})$
V_2O_5/SiO_2	3.7	3.3	2.0
$LiVO_3/SiO_2$	6.9	8.1	5.2
$NaVO_3/SiO_2$	15.2	15.4	34.4
KVO_3/SiO_2	6.2	5.6	9.2
$RbVO_3/SiO_2$	3.5	3.7	5.9
$CsVO_3/SiO_2$	5.4	5.3	14.5

Note. k, first-order rate constant.
[a] Related to the amount of the catalysts.
[b] Related to the BET surface area of the samples.
[c] Related to the amount of the surface V atoms.

vanadates decreased from Li to Cs, but the differences between $LiVO_3/SiO_2$ and $NaVO_3/SiO_2$ as well as between KVO_3/SiO_2 and $RbVO_3/SiO_2$ were negligible. On V_2O_5/SiO_2 the number of acidic sites was about 25% higher than on $LiVO_3/SiO_2$. The amount of adsorbed or irreversibly bonded CO_2, which is characteristic for the number of basic sites, increased significantly and nearly linearly as a function of cation radius from Li to Cs compounds.

2. Oxidation of Ethane on V_2O_5/SiO_2

We dealt earlier in great detail with the oxidation of ethane on silica-supported vanadia (12). With N_2O as oxidant, the main

oxidation products were ethylene, acetaldehyde, CO, and CO_2. Small amounts of CH_4, C_3, and C_4 hydrocarbons were also identified. The selectivities for ethylene and acetaldehyde formation at 823 K (conversion 5.2%) were 57.5% and 5.1%, respectively. With O_2 as oxidant, the same products were observed, but the conversion was higher and the selectivities lower.

3. Oxidation of Ethane on KVO_3/SiO_2

General features. Qualitatively the same oxidation products were found on alkali metal vanadate catalysts as on the mixed oxides. We discuss first the results obtained on KVO_3, which was studied in some detail.

TABLE 5

Some Characteristic Data for the Decomposition of C_2H_5OH on SiO_2-Supported V_2O_5 and Alkali Metal Vanadates at 580 K

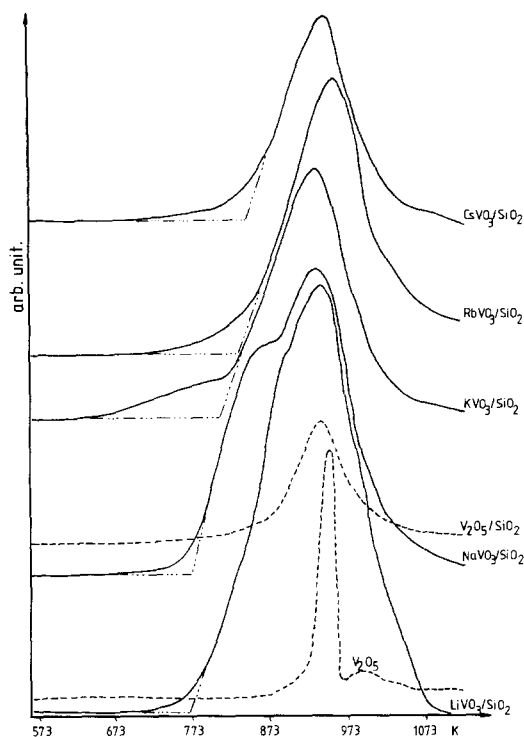|	Conversion (%)	Selectivity (%)			C_2H_x/CH_3CHO
		CH_3CHO	C_2H_4	C_2H_6	
V_2O_5/SiO_2	34.1	49.2	9.3	40.9	1.02
$LiVO_3/SiO_2$	16	56.7	3.1	38.4	0.73
$NaVO_3/SiO_2$	15.1	47.8	6.0	43.8	1.04
KVO_3/SiO_2	15.5	60.9	2.7	33.7	0.6
$RbVO_3/SiO_2$	12.5	54.2	2.8	41.4	0.82
$CsVO_3/SiO_2$	11.4	56.5	2.7	38.2	0.72

FIG. 10. The temperature-programmed reduction spectra of different alkali metal vanadates supported on SiO_2.

The basic differences between supported V_2O_5 and supported KVO_3 are: (i) there was no or only negligible decay in the conversion of ethane with time on KVO_3, and as a result the ethane conversion on KVO_3 was a factor of 1.8 greater than that measured on V_2O_5; (ii) the selectivities of acetaldehyde and CO_2 formation were considerably higher, and those of ethylene and CO production were lower.

Analysis of oxidation reaction data is generally based on the reduction–oxidation mechanism proposed by Mars and van Krevelen (32). The performance of an oxidation catalyst is closely related to its ability to take up and release oxygen. Catalysts with good reducibility exhibit high activities in full oxidation, but low selectivities in partial oxidation. Whereas O^{2-} or O species play a dominant role in the former case, in the latter case O^- and O_2^- can participate in the oxidation process.

Mechanism of the oxidation reaction. Previous studies on supported molybdenum oxide catalysts strongly suggested that O^- is the oxidizing agent in the partial oxidation of ethane (9). O^- is readily formed on vanadia-based catalysts, too: there is convincing evidence of the formation of O^- in the surface decomposition of N_2O (10). Note that O^- is not produced under the same conditions through O_2 adsorption (10). As concerns the catalytic effect of silica-supported V_2O_5 and vanadates, activated in vacuum at 773 K, we found that the decomposition of N_2O is fast on all samples above 673 K (Table 4). It is very likely that the active centres for the decomposition of N_2O are V^{4+} ions formed in the partial reduction of V^{5+} during vacuum treatment at 673 K. The occurrence of the following process can be presumed:

$$V^{4+} + N_2O = V^{5+} - O^- + N_2 \quad (1a)$$

$$2 V^{5+} - O^- = 2 V^{4+} + O_2. \quad (1b)$$
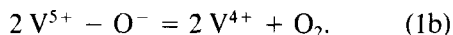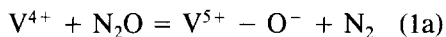
A mild reduction of the vanadate catalysts led to an enhancement of the rate of N_2O decomposition, possibly through an increase in the concentration of V^{4+}. Accordingly, V^{4+}, and hence the $V^{5+} - O^-$ surface

TABLE 6

Characteristic Data of the Temperature-Programmed Reduction of the SiO_2-Supported Alkali Metavanadates

Catalysts	T_i (K)	T_{max} (K)	O_{react} (μmol/g)	$M_2O \cdot V_2O_x$
V_2O_5	923	955		4,38
V_2O_5/SiO_2	865	940	122,1	3,8
$LiVO_3/SiO_2$	772	938	192,9	3.2
$NaVO_3/SiO_2$	773	933	167,2	3,5
KVO_3/SiO_2	795	933	110	3.9
$RbVO_3/SiO_2$	830	953	100,5	4.1
$CsVO_3/SiO_2$	840	943	62,9	4.4

Note. T_i, the onset temperature of the main reduction stage. T_{max}, the temperature of the TPR peak maxima. O_{react}, the amount of oxygen reacted.

species, are considered to be active centres in the partial oxidation of ethane.

In the oxidation of ethane, V^{4+} centres can be initially produced by the dissociation of V_2O_5 and by the reduction of V^{5+} ion by ethane at high reaction temperature, which is very likely a nonselective step

$$14 \ V^{5+} \ + \ 7 \ O^{2-} \ + \ C_2H_6 \rightarrow$$
$$14 \ V^{4+} \ + \ 2 \ CO_2 \ + \ 3 \ H_2O. \quad (2)$$
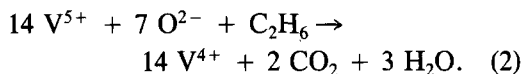
On the V^{4+} ion the N_2O decomposes to yield $V^{5+} - O^-$ surface species (Eq. (1)). In the subsequent steps, activation of the ethane molecule occurs, which involves the removal of a hydrogen atom by O^- to give the ethyl radical (9, 10, 12):
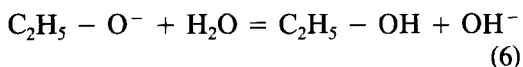
$$C_2H_6 \ + \ O^- \ = \ C_2H_5^* \ + \ OH^- \quad (3)$$

This surface species reacts further with O^- to form ethoxide:

$$C_2H_5^* \ + \ O^- \ = \ C_2H_5 \ - \ O^- \quad (4)$$
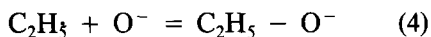
which can decompose to ethylene

$$C_2H_5 \ - \ O^- \ = \ C_2H_4 \ + \ OH^- \quad (5)$$

or react with H_2O to produce ethanol

$$C_2H_5 \ - \ O^- \ + \ H_2O \ = \ C_2H_5 \ - \ OH \ + \ OH^- \quad (6)$$

or with OH groups to yield acetaldehyde

$$2 \ V^{5+} \ + \ C_2H_5 \ - \ O^- \ + \ OH^-$$
$$= \ CH_3 \ - \ CHO \ + \ H_2O \ + \ 2 \ V^{4+}. \quad (7)$$
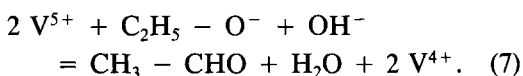
As more acetaldehyde is produced in the decomposition of ethanol than hydrocarbons on alkali metal vanadates, the transitory formation of ethanol is also favourable for acetaldehyde production.

As regards the importance of these steps in the present case, we can rely on the results of our supplementary measurements. The pulse experiments indicated that C_2H_6 exhibited little reactivity towards KVO_3 at 823 K (less than 0.5% of the ethane pulse reacted with KVO_3) and produced very few V^{4+} centres active in the decomposition of N_2O (less than 0.5% of the N_2O pulse decomposed). In other words, the reaction be-

tween O^{2-} of KVO_3 and C_2H_6, involving among other processes the abstraction of a hydrogen atom, is slow at 823 K. This is in contrast with V_2O_5 catalyst, where this reaction occurred more easily at that temperature (12). Treatment of KVO_3 with N_2O pulses at 823 K enhanced the extent of the reaction of subsequent pulses of C_2H_6 only slightly. As N_2O decomposes on KVO_3 at 823 K, this result means that the O^- produced in the decomposition is not stable on KVO_3 at such a high temperature and desorbs in the form of O_2. This feature is in harmony with the observation of Iwamatsu et al. (10), whose ESR measurements demonstrated that O^- is unstable on V_2O_5/SiO_2 above 373 K. The reaction between C_2H_6 and N_2O on KVO_3 was greatly facilitated by CO treatment at 823 K, very probably due to the enhanced production of V^{4+}, and hence to the formation of O^- centres. Interestingly, the development of an active phase of KVO_3 can also be achieved by the reacting gas mixture: after the admission of five pulses of C_2H_6–N_2O onto the catalyst, the same high activity and selectivity were attained as observed following CO treatment (Fig. 9). This suggests that in the oxidation of C_2H_6 a more reactive intermediate is formed for the activation of the catalyst, i.e., for the formation of V^{4+}.

This species is very likely to be the ethyl radical, which can reduce V^{5+} to V^{4+}. Ethyl radical was detected by ESR measurements following irradiation of MoO_3/SiO_2 catalyst (33); it exhibited high reactivity even at low temperature.

Attempts to detect $C_2H_5 \ - \ O^-$ species during the oxidation by means of IR spectroscopy were hampered by the low transmission of our silica-supported catalyst in the region 1000–1200 cm^{-1}. However, as C_2H_5OH was found among the reaction products, and this adsorbs and decomposes through $C_2H_5O^-$ formation (34), we can reckon with its existence on our catalyst sample, too. Study of the decomposition of ethanol on vanadate samples verified steps 5 and 7: acetaldehyde and ethylene were

formed in large quantities. (Most of the ethylene reacted with hydrogen, formed in the alcohol decomposition, to give ethane.) The increase in selectivity towards CH_3CHO in the selective oxidation of ethane in the presence of H_2O (Table 3) may be accounted for by reaction 5.

Since the decomposition of ethanol and ethoxide to ethylene occurs on the acidic sites of the catalyst, and this is greatly decreased from V_2O_5/SiO_2 to KVO_3/SiO_2 the difference in the selectivities of acetaldehyde and ethylene production on KVO_3 as compared to V_2O_5 may be associated with this property of KVO_3. In harmony with this, the formation of CH_3CHO in the decomposition of C_2H_5OH was also more considerable on KVO_3/SiO_2 than on V_2O_5/SiO_2. The other products of the oxidation, CO_2 and CO, are very probably produced in the decomposition and/or oxidation of acetaldehyde. It may also be assumed that acetaldehyde is more stable on KVO_3 than on V_2O_5, and therefore less CO is formed.

In the presence of water the selectivity of acetaldehyde is greatly increased (Figs. 2, 8, and 9). This effect can probably be attributed to the increase of the concentration of surface OH groups (Eq. (7)). We note here that in the presence of water the value of the activation energy for ethane conversion is considerably higher than that measured in the absence of water. In that context we mention that the tetrahedral environment of vanadium in KVO_3 becomes octahedrally coordinated when it interacts with water (30). This structural change can cause an increase in the activation energy as was found in the alcohol decomposition on tri- and hexavanadates (15).

4. Comparison of the Catalytic Behaviour of Alkali Metal Vanadates

In general, all the alkali metal vanadates behaved similarly. In detail, however, there were differences particularly in the stability and selectivity of the catalysts. As regards the conversion of ethane oxidation and the rates relating to the number of surface V

ions, there is no systematic change as a function of the size of alkali metal ions. There is also no correlation between reducibility and activity of the catalysts (Tables 3 and 6).

An enhanced selectivity towards acetaldehyde production relative to that on V_2O_5 was observed on all alkali metal vanadates; moreover, the initial selectivity was higher. The sequence of initial selectivity was $Cs = Rb > K > Na > Li$. However, in contrast with KVO_3, the selectivity of acetaldehyde formation on the other vanadates underwent a significant decrease and, as a result, after 3–4 h the highest value was measured on KVO_3 (Fig. 8). As mentioned above, $NaVO_3$ decomposed at the temperature of the reaction (which resulted in a drastic loss in its catalytic performance), and therefore its behaviour cannot be compared with that of the other alkali metal vanadates. As the number of acidic sites on the silica-supported alkali metal vanadates decreased, and the number of basic sites increased in the sequence Li–Na–K–Rb–Cs (Table 1), the selectivity sequence for CH_3CHO production is very probably connected with these properties.

As regards the selectivity of ethylene formation, the highest value (45–47%) was found on $LiVO_3$. This was followed by K, Rb, and Cs. Interestingly, the selectivity of ethylene formation remained practically the same during the 5-h catalytic run. From the parallel changes of the acidic nature of the catalysts and the selectivity of the ethylene production (Tables 1 and 3) we may conclude that the ethylene formation proceeds on the acidic sites of vanadates.

The above sequence of the selectivities of alkali metal vanadates remained the same in the presence of H_2O, with the significant difference that the selectivity of CH_3CHO formation was markedly higher and did not decay with time.

REFERENCES

1. Boreskov, G. K., in "Advances in Catalysis" (D. D. Eley, P. W. Selwood, and P. B. Weisz, Eds.), Vol. 15, p. 279. Academic Press, New York, 1964.

2. Dzisjak, A. P., Boreskov, G. K., Kasatkina, L. A., and Kochurihin, V. E., *Kinet. Katal.* **2,** 386 (1961).

3. Krupay, B. W., and Ross, R. A., *J. Catal.* **50,** 220 (1977).

4. Bibin, V. N., and Kasatkina, L. A., *Kinet. Katal.* **5,** 734 (1964).

5. Milisavlevich, B. S., Ivanov, A. A., Polyakova, G. M., and Serzhantova, V. V., *Kinet. Katal.* **16,** 103 (1975).

6. Jiru P., and Jara V., *in* "Proceedings, 2nd International Congress on Catalysis, Paris, 1960," p. 2113. Technip, Paris, 1961.

7. Thorsteison, E. M., Wilson, T. P., Young, F. G., and Kasai, P. H., *J. Catal.* **52,** 116 (1978).

8. Iwamoto, M., Taga, T., and Kagawa, S., *Chem. Lett.,* 1469 (1982).

9. Mendelovici, L., and Lunsford, J. H., *J. Catal.* **94,** 37 (1985).

10. Iwamatsu, E., Aika, K., and Onishi, T., *Bull. Chem. Soc. Jpn.* **59,** 1665 (1986).

11. Erdőhelyi, A., and Solymosi, F. *Appl. Catal.* **39,** L11 (1988).

12. Erdőhelyi, A., and Solymosi, F. *J. Catal.* **123,** 31 (1990).

13. Kera, Y., *in* "Proceedings, 7th International Congress on Catalysis, Tokyo, 1980" (T. Seiyama and K. Tanabe, Eds.), p. 1400. Elsevier, Amsterdam, 1981.

14. Kera, Y., *Bull. Chem. Soc. Jpn.* **54,** 1693 (1981).

15. Kera, Y., and Negro, M., *J. Catal.* **99,** 198 (1986).

16. Fricke, R., Hanke, W., Jerschkiewitz, H.-G., Parlitz, B., and Öhlmann, G., *Appl. Catal.* **9,** 235 (1984).

17. Gmelin Handbuch V B2 371, B2 416, B2 486, B2 494.

18. Solymosi, F., Erdőhelyi, A., and Bànsàgi, T., *J.*

Catal. **68,** 371 (1981); Erdőhelyi, A., and Solymosi, F., *J. Catal.* **84,** 446 (1983).

19. Oyama, S. T., Lewis, K. B., Carr, A. M., and Somorjai, G. A., *in* "Proceedings, 9th International Congress on Catalysis, Calgary, 1988" (M. J. Phillips and M. Ternan, Eds.), Vol. 3, p. 1489, Chem. Institute of Canada, Ottawa, 1988; Oyama, S. T., Went, G. T., Lewis, K. B., Bell, A. T., and Somorjai, G. A., *J. Phys. Chem.* **93,** 6786 (1989).

20. Ai, M., *J. Catal.* **54,** 223 (1978).

21. Tanabe, K., "Solid Acid and Bases." Kodansha, Tokyo and Academic Press, New York, 1970.

22. Gilde, S. A., Erdőhelyi, A., and Solymosi, F., in press.

23. Monti, D., Reller, A., and Baiker, A., *J. Catal.* **93,** 360 (1985).

24. Klissurski, D., and Abadzhijeva, N., *React. Kinet. Catal. Lett.* **2,** 431 (1975).

25. Ng, H. N., Calvo, C., and Idler, K. L., *J. Solid State Chem.* **27,** 357 (1979).

26. Hawthorne, F. C., and Calvo, C., *J. Solid State Chem.* **22,** 157 (1977).

27. Bubnova, R. S., and Filatova, S. K., *Izv. Akad. Nauk, SSSR Neorg. Mater.* **24,** 1525 (1988).

28. Evans, H. T., *Z. Kristallogr.* **114,** 257 (1960).

29. Christ, C. L., Clark, J. R., and Evans, H. T., *Acta Crystallogr.* **7,** 801 (1954).

30. Mastikhin, V. M., Lapina, O. B., and Simonova, L. G., *React. Kinet. Catal. Lett.* **24,** 127 (1984).

31. Neumann, B., and Sonntag, A., *Z. Elektrochem.* **41,** 860 (1935).

32. Mars, P., and van Krevelen, D. W., *Chem. Eng. Sci. Spec. Suppl.* **3,** 41 (1954).

33. Kaliaguine, S. L., Shelimov, B. N., and Kazansky, V. B., *J. Catal.* **55,** 384 (1978).

34. Sugioka, M., Kamanaka, T., and Aomura, K., *J. Catal.* **52,** 531 (1978).